Use of Low/Mid-Temperature Solar Heat for Thermochemical Upgrading of Energy, Part I: Application to a Novel Chemically-Recuperated Gas-Turbine Power Generation (SOLRGT) System

Na Zhang[1]
Institute of Engineering Thermophysics,
Chinese Academy of Sciences,
Beijing, 100190, P. R. C.
e-mail: zhangna@mail.etp.ac.cn

Noam Lior
Department of Mechanical Engineering
and Applied Mechanics,
University of Pennsylvania,
Philadelphia, PA 19104-6315

This paper is the first part of a study presenting the concept of indirect thermochemical upgrading of low/mid temperature solar heat, and demonstration of its integration into a high efficiency novel hybrid power generation system. The proposed system consists of an intercooled chemically recuperated gas turbine (SOLRGT) cycle, in which the solar thermal energy collected at about 220 °C is first transformed into the latent heat of vapor supplied to a reformer and then via the reforming reactions to the produced syngas chemical exergy. The produced syngas is burned to provide high temperature working fluid to a gas turbine. The solar-driven steam production helps to improve both the chemical and thermal recuperation in the system. Using well established technologies including steam reforming and low/mid temperature solar heat collection, the hybrid system exhibits promising performance: the net solar-to-electricity efficiency, based on the gross solar thermal energy incident on the collector, was predicted to be 25–30%, and up to 38% when the solar share is reduced. In comparison to a conventional CRGT system, 20% of fossil fuel saving is feasible with the solar thermal share of 22%, and the system overall efficiency reaches 51.2% to 53.6% when the solar thermal share is increased from 11 to 28.8%. The overall efficiency is about 5.6%-points higher than that of a comparable intercooled CRGT system without solar assist. Production of NO_x is near zero, and the reduction of fossil fuel use results in a commensurate ~20% reduction of CO_2 emissions. Comparison of the fuel-based efficiencies of the SOLRGT and a conventional commercial Combined Cycle (CC) shows that the efficiency of SOLRGT becomes higher than that of CC when the solar thermal fraction X_{sol} is above ~14%, and since the SOLRGT system thus uses up to 12% less fossil fuel than the CC (within the parameter range of this study), it commensurately reduces CO_2 emissions and saves depletable fossil fuel. An economic analysis of SOLRGT shows that the generated electricity cost by the system is about 0.06 $/kWh, and the payback period about 10.7 years (including 2 years of construction). The second part of the study is a separate paper (Part II) describing an advancement of this system guided by the exergy analysis of SOLRGT. [DOI: 10.1115/1.4006083]

Keywords: hybrid power system, solar heat, thermochemical exergy upgrading, chemically recuperated gas turbine, fossil fuel saving

1 Introduction

Conventionally, solar applications for lower temperature of about 200 °C and less are principally for space heating and for drying. Power generation from such low temperature solar heat obviously has low efficiency. For example, in Rankine cycle systems using organic working fluids, the top temperature is typically limited anyway by the organic fluids boiling temperature and deterioration at higher temperature superheat, resulting in cycle efficiency generally lower than 10%. To raise the thermo-economic efficiency, hybrid systems were introduced that use multiple heat sources at different temperature levels in a way that low-temperature, and thus low exergy, sources are used when they are inexpensive, and higher temperature sources are integrated according to their cost to raise the energy efficiency. Probably the earliest such hybrid system was introduced by Lior and coworkers [1–5] where solar heat at temperatures below ~100 °C, produced by flat-plate solar collectors at relatively low cost, is used as the largest energy input, and fossil fuel or concentrating solar collector heat input at higher temperatures is added for efficiency improvement. A configuration of such a system (named SSPRE: "Solar Steam Powered Rankine Engine) [1–5] used steam as the working fluid, where nearly 80% of the heat was supplied by solar collectors at ~100 °C to provide the latent heat for boiling the water, and the remaining 20% was supplied from higher

[1]Corresponding author.

Contributed by the International Gas Turbine Institute (IGTI) of ASME for publication in the JOURNAL OF ENGINEERING FOR GAS TURBINES AND POWER. Manuscript received January 21, 2012; final manuscript received February 1, 2012; published online May 23, 2012. Editor: Dilip R. Ballal.

temperature energy sources for superheating the steam up to ~600 °C, thus doubling the cycle efficiency to about 18%, as compared with organic (or other working fluid) Rankine cycles which operate at similar solar collector temperatures. The increased efficiency thus reduces the system cost significantly because only about half of the solar collector area is required, collectors that are cheaper than concentrating collectors to begin with. It is noteworthy that the same hybrid solar system principle (but at higher temperatures, using solar concentrating collectors) was later adopted by most of the operating and proposed solar thermal power systems, such as those by Luz, Solel, and the "DESERTEC" proposal [6–15]. Their efficiency is, however, still relatively low because the designers have chosen relatively low top temperatures and pressures. Starting from the premise that the cost of solar heat increases with the temperature at which it is delivered, we are exploring the idea that instead of applying the solar heat at very high temperatures, it is used at low/mid temperatures to contribute to the production of fossil fuels that can then be burned to produce heat at the high temperature that can generate power in high efficiency conversion systems, such as gas turbines and fuel cells. It is generally possible to integrate solar heat input into some heat absorption process in power plants either thermally, such as in evaporation (as done in the above-mentioned SSPRE system) and in the recuperation process, or thermochemically, such as in some endothermic reactions like reforming and decomposition. In the power system, thermal integration converts the absorbed solar heat into internal heat of the working fluid; however, thermo-chemical integration converts the absorbed solar heat into the working fluid chemical energy, thus achieving the upgrading of the solar heat. Methanol-steam reforming and methanol decomposition can achieve over 90% conversion into hydrogen-rich syngas at temperature of about 250 °C. Taking advantage of high conversion rates at the relatively low temperature of about 250 °C, Hong, Jin and co-workers [16,17] proposed a combined cycle (named Solar CC) that ingeniously integrates mid-temperature solar thermal energy with methanol decomposition. Solar heat at 200–300 °C supplies the heat for the endothermic reaction of methanol decomposition into syngas, and is thereby converted to its chemical energy. This produced syngas is used as the fuel in the combustor of a topping Brayton cycle, and the Brayton cycle exhaust drives a dual-pressure Rankine bottoming cycle to produce additional power. In this way, the low temperature solar heat is upgraded and released as high temperature thermal energy for power generation. In a case study in Ref. [16], the system efficiency of the hybrid combined cycle (defined as the net power output divided by the summation of the fuel lower heating value and the absorbed solar exergy) is 60.7%. The solar heat share in the system input is 18%, and the solar-to-power net efficiency (refer to Eq. (28)) can reach 35%. This analysis, however, is based on simplified models without accounting for turbine blade cooling requirements, which affect cycle performance. The same authors also proposed a hybrid combined cycle employing methane-fuel chemical-looping combustion [18], in which solar thermal energy at 450–550 °C is used to drive the endothermic reaction of methane fuel with NiO in the reduction reactor, accomplishing also CO_2 capture with low energy penalty by chemical-looping combustion.

Methane is, however, a more widely used fuel than methanol, and furthermore, the enthalpy rise in the methane-steam reforming reaction is 165 kJ/mol, higher than the 49.5 kJ/mol in methanol-steam reforming and the 90.7 kJ/mol in methanol decomposition, and therefore has a larger heat absorption potential. The methane-steam reforming reaction requires, however, a much higher temperature, of above 800 °C with Ni-based catalyst to obtain reasonably high methane conversion. For this reason, the state of the art of solar thermo-chemical technology is principally focused on the use of high temperature solar heat, such as solar steam reforming of natural gas (methane), at about 900–1000 °C [19]. The methane conversion does not even occur under 327 °C (600 K) [20]. Low temperature solar heat at about 200 °C-300 °C therefore does not match the direct application in this case. To use this low temperature solar heat and to achieve its chemical conversion with methane-steam reforming, an indirect way has to be worked out.

In this paper, indirect upgrading of low/mid temperature solar heat is proposed. Rather than driving the endothermic reforming reaction directly, the solar heat is used to evaporate water, at a relatively low temperature, for generating the steam needed for methane reforming. Thus the low/mid temperature solar heat is first transformed to the vapor latent heat, and then it is further transformed to the syngas chemical energy via the reforming reaction, enabling this upgraded generated fuel to be burned and used in a high efficiency power generation system. A hybrid solar assisted chemically recuperated gas turbine (SOLRGT) system first introduced in Ref. [21] is proposed to embody this concept of indirect upgrading of solar heat. As shown below, the same electricity output as that generated by a conventional chemically recuperated gas turbine (CRGT) system without solar heat contribution is attained with about 20% less fuel input. An economic analysis of SOLRGT shows that the generated electricity cost by the system is about 0.06 $/kWh, and the payback period about 10.7 years (including two years of construction). The features of the system integration are identified and the feasibility of indirect upgrading of solar heat is demonstrated.

2 Indirect Upgrading the Low/Mid Temperature Solar Heat

Figure 1 illustrates the two-step indirect upgrading of the low/mid temperature solar heat.

2.1 From Solar Heat to Steam Internal Heat. In the steam generation process driven by solar heat, the water absorbs solar heat and converts it into the steam internal heat. The subscripts *w*, *s*, sol represent the water, steam and solar heat, respectively. The energy balance and exergy balance for the steam generation process are:

$$\Delta H_w + Q_{\mathrm{sol}} = \Delta H_s \tag{1}$$

$$\Delta E_w + \Delta E_{\mathrm{sol}} = \Delta E_s + \Delta EXL_1 \tag{2}$$

where ΔEXL_1 is the exergy loss in the steam generation process. ΔH contains both chemical and thermal energy, and ΔE contains both chemical and thermal exergy. Following Ishida and coworkers [22,23], an "energy level" A is defined for any energy transformation process as the ratio of the changes of the exergy and the enthalpy in the process, as:

$$\Delta E_w = \Delta H_w A_w \tag{3}$$

$$\Delta E_{\mathrm{sol}} = Q_{\mathrm{sol}} A_{\mathrm{sol}} \tag{4}$$

$$\Delta E_s = \Delta H_s A_s \tag{5}$$

ΔEXL_1 represents the exergy destruction caused by the energy level difference between the solar heat provide by the collector A_{sol} and the steam generation heat A_{sg}, caused by the temperature difference of the heat donation and acceptance.

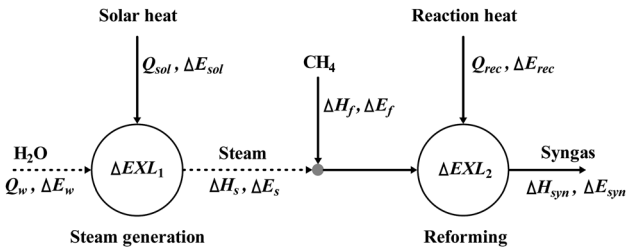

Fig. 1 Indirect upgrading the low/mid level solar heat

$$\Delta EXL_1 = Q_{\text{sol}}(A_{\text{sol}} - A_{sg}) \tag{6}$$

Substituting Eqs. (3)–(6) into Eq. (2) gives

$$\Delta H_s A_s = \Delta H_w A_w + Q_{\text{sol}} A_{sg} \tag{7}$$

Introducing Eq. (1) into Eq. (7) gives:

$$Q_{\text{sol}} A_s = \Delta H_w (A_w - A_s) + Q_{\text{sol}} A_{sg} \tag{8}$$

Subtracting the solar thermal exergy $Q_{\text{sol}}A_{\text{sol}}$ on both sides of Eq. (8) gives:

$$Q_{\text{sol}}(A_s - A_{\text{sol}}) = \Delta H_w (A_w - A_s) - Q_{\text{sol}}(A_{\text{sol}} - A_{sg}) \tag{9}$$

and it further gives:

$$A_s - A_{\text{sol}} = -\frac{\Delta H_w}{Q_{\text{sol}}}(A_s - A_w) - (A_{\text{sol}} - A_{sg}) \tag{10}$$

Since the energy level of steam is higher than that of water, and the energy level of solar heat is higher than the steam generation heat, i.e., $A_s > A_w$ and $A_{\text{sol}} > A_{sg}$, therefore the right side of Eq. (10) has a negative value, which means that the energy level of the solar heat drops in the steam generation process, and actually the solar heat exergy is destroyed in any thermal integration process because of the required heat transfer temperature difference.

2.2 From Steam Internal Heat to Syngas Chemical Exergy. The reformer has a key role in the solar heat upgrading, its inflows are the natural gas and the steam, and the outflow is the syngas, the flows are denoted with the subscript *f*, *s*, and syn, respectively, and the reforming reaction receives heat Q_{rec} from an external heat source (such as the turbine exhaust heat recuperation in this paper). The energy conservation and the exergy balance are, respectively, given by Eqs. (11) and (12):

$$\Delta H_f + \Delta H_s + Q_{\text{rec}} = \Delta H_{\text{syn}} \tag{11}$$

$$\Delta E_f + \Delta E_s + \Delta E_{\text{rec}} = \Delta E_{\text{syn}} + \Delta EXL_2 \tag{12}$$

where ΔEXL_2 is the exergy loss in the reforming process. The following equations are obtained based on the concept of energy level *A*:

$$\Delta E_f = \Delta H_f A_f \tag{13}$$

$$\Delta E_s = \Delta H_s A_s \tag{14}$$

$$\Delta E_{\text{rec}} = Q_{\text{rec}} A_{ex} \tag{15}$$

$$\Delta E_{\text{syn}} = \Delta H_{\text{syn}} A_{\text{syn}} \tag{16}$$

ΔEXL_2 represents the exergy destruction caused by the energy level difference between the external source heat entered into the reformer and the reaction heat in the reformer, caused by the temperature difference of the heat donation and acceptance [16,17].

$$\Delta EXL_2 = Q_{\text{rec}}(A_{ex} - A_{\text{rec}}) \tag{17}$$

where A_{ex} is the energy level of the external heat for the reforming, and A_{rec} is the energy level of the reaction heat.

Substituting Eqs. (11) and (13)–(17) into Eq. (12), we obtain:

$$\Delta H_f A_f + \Delta H_s A_s + Q_{\text{rec}} A_{ex} = (\Delta H_f + \Delta H_s + Q_{\text{rec}}) A_{\text{syn}} + Q_{\text{rec}}(A_{ex} - A_{\text{rec}}) \tag{18}$$

It further gives:

$$\Delta H_f (A_f - A_{\text{syn}}) = \Delta H_s (A_{\text{syn}} - A_s) + Q_{\text{rec}}(A_{\text{syn}} - A_{\text{rec}}) \tag{19}$$

Equation (9) shows the upgrading of both the steam energy level $(A_{\text{syn}} - A_s)$ and the absorbed external heat energy level $(A_{\text{syn}} - A_{\text{rec}})$, which means that the reforming reaction boosts both the reacted steam energy and the external heat energy level to a much higher syngas chemical energy level, with the degradation of energy level of fuel from methane to syngas $(A_f - A_{\text{syn}})$ serves as the driving force. Since the low/mid temperature solar heat is absorbed as the vapor latent heat, it accomplishes the energy level upgrading indirectly. The steam energy level increases from A_s to A_{syn} and can be written as:

$$A_{\text{syn}} - A_s = \frac{\Delta H_f}{\Delta H_s}(A_f - A_{\text{syn}}) - \frac{Q_{\text{rec}}}{\Delta H_s}(A_{\text{syn}} - A_{\text{rec}}) \tag{20}$$

From Eq. (10) and (20), the upgrading of the energy level of solar heat can be expressed as:

$$A_{\text{syn}} - A_{\text{sol}} = \frac{\Delta H_f}{\Delta H_s}(A_f - A_{\text{syn}}) - \frac{Q_{\text{rec}}}{\Delta H_s}(A_{\text{syn}} - A_{\text{rec}}) - \frac{\Delta H_w}{Q_{\text{sol}}}(A_s - A_w) - (A_{\text{sol}} - A_{sg}) \tag{21}$$

The fuel enthalpy input ΔH_f is approximately equal to its lower heating value input Q_f, which is much higher than the reforming heat Q_{rec} and the water enthalpy ΔH_w; the energy level *A* of methane is about 1.05, the average reaction heat energy level A_{rec} is about 0.6 driven by turbine exhaust heat with the temperature of 500 °C (average temperature inside the reformer), and the syngas fuel has an energy level of about 0.83–0.9 depending on the composition [17]. In other words, the energy level differences $(A_f - A_{\text{syn}})$ and $(A_{\text{syn}} - A_{\text{rec}})$ are roughly of the same order. $(A_s - A_w)$ and $(A_{\text{sol}} - A_{sg})$ are relatively smaller because of the small temperature difference between saturated steam and water, and between solar heat and the steam generation process absorbed heat. Therefore, the first term on the right side of Eq. (21) is much larger than other terms, ensuring a positive value to $(A_{\text{syn}} - A_{\text{sol}})$. Since the energy level for the solar heat can be expressed as $A_{\text{sol}} = (1 - T_0/T_{\text{sol}})$, and it is near 0.4 at solar heat temperature T_{sol} of 220 °C, the relative indirect upgrade in solar heat energy level $(A_{\text{syn}} - A_{\text{sol}})/A_{\text{sol}}$ is about 1.2. From the above discussion, we see that the thermal integration with solar heat decreases its energy level, and that the energy level of solar heat can be upgraded only by thermo-chemical integration.

3 System Configuration Description

3.1 The Basic CRGT System. In the chemically recuperated gas turbine CRGT [20,24–27] system shown in Fig. 2, the turbine exhaust heat is recovered in a heat recovery steam generator

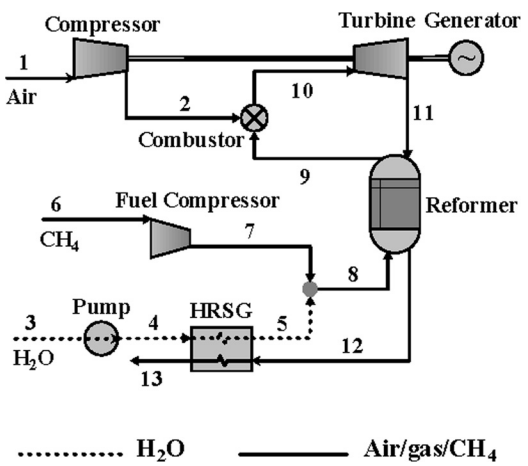

Fig. 2 Schematic diagram of the basic CRGT cycle

(HRSG), the superheater section of which is replaced by a methane steam reformer. The natural gas reforming process takes heat from the turbine exhaust to produce hydrogen-rich syngas, thus converting some of the turbine exhaust heat into the reforming products heating value, thereby increasing the power generation and efficiency beyond that with direct combustion alone. Another key advantage of CRGT cycles is their potential to produce ultra-low NO_x emissions, estimated to be as low as 1 ppm [20,24], compared with 25 ppm from the steam-injected gas turbine cycle (STIG), due to the presence in the CRGT of a significant amount of steam in the produced syngas, which lowers the temperature in the primary zone of the gas turbine combustor and prevents formation of much thermal NO_x, while the presence of hydrogen in the syngas extends the flammability limits to these low temperatures. We also note that a comparison conducted by Kesser et al. [24] concluded that the basic CRGT cycle (without intercooling or reheat) has a thermal efficiency higher than the STIG cycle and the simple gas turbine cycle, but not as high as the combined cycle.

The reforming process is characterized by the following main reactions [20]:

$$CH_4 + H_2O \leftrightarrow CO + 3H_2 \qquad \Delta H = 206.11\ \text{kJ/mol}$$
$$CO + H_2O \leftrightarrow CO_2 + H_2 \qquad \Delta H = -41.17\ \text{kJ/mol}$$

The first reaction is the methane reforming. The methane/steam mixture absorbs heat thermally and also chemically via the endothermic reaction processes, resulting in a larger exhaust heat recuperation capacity than conventional thermal recuperation alone as demonstrated by the additional reaction heat demand shown in the above equations. Moreover, 20–50% conversion is realizable using turbine exhaust heat at 600 °C (turbine exit state point), with the methane conversion increasing with higher steam addition and temperature and lower pressure. The second of the above-shown reactions is known as the shift reaction, which is exothermic and is therefore undesirable since it reduces the net endothermicity.

3.2 The Solar Improved CRGT Cycle. The two-step indirect solar upgrading is demonstrated with the solar heat improved chemically recuperated gas turbine (SOLRGT) cycle proposed in this paper as depicted in Fig. 3, in which the reforming water is evaporated by low/mid temperature solar heat. In that way, the low/mid temperature solar heat assists in generating syngas chemical energy in the reforming process, and finally converts to electricity in the high temperature gas turbine system. Different also from the CRGT cycle in Fig. 2, compressor intercooling is employed to reduce the compression power demand; and with the assistance of solar heat, more turbine exhaust heat is thus available to allow recuperation to preheat the cold compressed air.

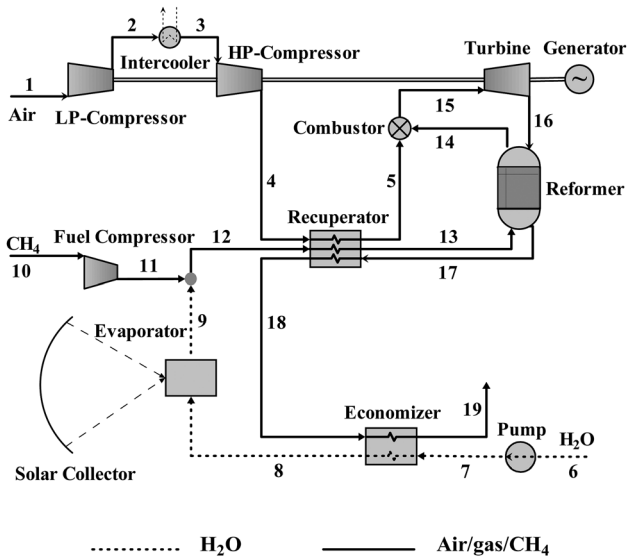

Fig. 3 Schematic diagram of the SOLRGT cycle

Features of the SOLRGT system that contribute in an important way to its high efficiency include:

(1) In comparison with the direct solar heated methane steam reforming that requires solar heat at temperatures above 800 °C, the proposed SOLRGT system employs solar heat at only, 200–250 °C. These much lower temperatures allow the use of cheaper and more efficient solar collectors. We also note that this type of hybrid cycle retains its thermodynamic advantages when used with any low-temperature energy sources, such as waste or geothermal heat, and its CO_2 emission reduction advantages when the heat sources do not generate CO_2.
(2) The temperature match in the turbine exhaust heat recuperation process can be improved significantly since it releases heat only to a sensible heat sink with varying temperature; thus resulting in a significant reduction of the associated heat transfer related exergy destruction, eliminating at the same time the approach-temperature-difference constraint in the evaporator and thus more steam can be produced.
(3) It allows the recuperation to heat the compressed air prior to its inlet to the combustor. The basic CRGT cycle thermal efficiency increases with the steam-air mass ratio, and thus the highest efficiency is obtained when all the turbine exhaust heat is used for steam generation in the HRSG, thus leaving none for preheating the compressed air. In the proposed SOLRGT system, solar heat provides the latent heat for the water evaporation and thus higher temperature turbine exhaust heat can be used for the compressed air preheating. This reduces fuel consumption and elevates the thermal efficiency.
(4) It allows compression with intercooling and a high steam-methane mole ratio simultaneously. The adoption of intercooling reduces the compressor power consumption and the need for turbine blade cooling. At the same time, it generally reduces the efficiency since colder compressed working fluid demands higher fuel input, but this negative effect on efficiency can be eliminated if compressed air recuperation is adopted at the same time (as we do in SOLRGT). As the fuel demand increases, the steam flow rate needs be increased proportionally to maintain the same steam-methane ratio. In contrast, the conventional CRGT cycle with intercooling of a given *TIT* and expansion ratio does not produce enough turbine exhaust heat to generate the required additional amount of steam, and thus the steam-methane mole ratio decreases, which in turn decreases the methane conversion in the reformer and lowers the benefit of the chemical recuperation [20]. In the proposed SOLRGT system, the use of solar heat allows even more steam to be generated for achieving a higher steam-methane ratio. Compressor inter-cooling helps to recuperate more turbine exhaust heat, leading to a lower heat rejection to the environment, and thus all the positive impacts of intercooling are retained and both negative impacts (on efficiency and on steam-methane mole ratio) are eliminated in the new system.

4 The Computation Model and its Validation

4.1 The Gas Turbine Cooling Model. High temperature gas turbine performance levels are very sensitive to blade cooling requirements. To analyze the global performance of the cycle that we are investigating, a discrete (rather than differential field) model was used because it is computationally more convenient. For this study, we considered the cooled turbine model presented in Ref. [20], which was original published by Stecco and Facchini [28].

In such a discrete model, the expansion path was reduced to a number of discrete elementary operations, in which the gas expansion process in the turbine includes several mixing processes between the expanding hot gas and the fluid streams added for blade cooling. It considers the turbine stage-by-stage, and estimates the cooling flow necessary for the stator and rotor of each stage. The stator flow is assumed to mix with the main gas flow prior to flow through the turbine, i.e., the mixing happens before the power extraction. The rotor coolant flow is mixed into the main stream at the rotor exit (after the power extraction).

For each cooling step, the required coolant mass flow is calculated using:

$$\frac{m_c}{m_g} = \frac{C_{pg}}{C_{pc}} St_g \frac{A_b}{A_g} \frac{1}{\varepsilon_c} \frac{\phi}{1-\phi} \tag{22}$$

where subscripts g and c refer to the main gas stream and the cooling stream, respectively. St_g is main gas Stanton number, F_b is the blade surface area, F_g is the flue gas path cross-sectional area, ε_c is the cooling efficiency.

The cooling effectiveness ϕ is defined as:

$$\phi = (T_g - T_b)/(T_g - T_c) \tag{23}$$

For an advanced power generation gas turbine, commonly used values for St_g, A_b/A_g and ε_c are 0.005, 4 and 0.3 [29]. T_b refers to the turbine blade metal temperature; its value in this study is 1093 K (820 °C) and is kept constant in the calculation, which is validated by calibrating the model against the published performance data of a basic CRGT cycle in Ref. [24]. The turbine in the SOLRGT cycle is divided into four stages assuming equal enthalpy drops and the first two stages are cooled.

4.2 Main Assumptions for the Simulation. The cycles are simulated using ASPEN PLUS process simulation software [30], in which the component models are based on the energy balance and mass balance and species balance, with the default relative convergence error tolerance of 0.01%, which is the specified tolerance for all tear convergence variables [30]. The RK-Soave thermodynamic model was selected for the thermal property calculations. The reformer (REF) has been simulated by the Gibbs Reactor available in the ASPEN PLUS model library, which determines the equilibrium conditions by minimizing Gibbs free energy. The chemical non-equilibrium effects in REF due to reaction kinetics are modeled using the chemical approach to equilibrium ΔT_{eq} [20,24], which indicates how close a reaction is to reaching equilibrium. The syngas composition at the exit of the reformer is thus the equilibrium composition at temperature of $(T - \Delta T_{eq})$. The most relevant assumptions are summarized in Table 1.

4.3 Model Validation. To validate the computation model, a basic CRGT cycle as shown in Fig. 2 was simulated (referred as case A) and compared with the computation done by Kesser et al. [24]. Table 2 reports the main results of the comparison. The parameters from the computations by Kesser et al. [24] (shown with the superscript "a" in Table 2, including the inflow state parameters, compressor and turbine efficiencies, and heat transfer temperature differences) were used as the input data in our simulation. Keeping a constant steam/methane ratio of 6.1, the fuel mass flow rate was varied to obtain a combustor exit temperature of 1308 °C; the syngas composition, the system thermal efficiency, the specific power output and the cooling air fraction were calculated. As shown in Table 2, good agreement of the results was obtained, with the most notable difference being the turbine exit temperature. We obtained a slightly lower turbine exit temperature, leading to a slightly lower reformer exit temperature for the same heat transfer temperature difference in REF, resulting in a slightly lower methane conversion rate and very slightly lower system efficiency.

5 System Performance Analysis and Comparison

5.1 Performance Criteria. The thermal efficiency of the system is defined as:

$$\eta_{th} = \frac{W_{\text{net}}}{Q_f + Q_{\text{sol}}} = \frac{W_{\text{net}}}{m_f \cdot LHV + Q_{\text{sol}}} \tag{24}$$

Table 1 Main assumptions for the calculation

			Source
Compressor	Pressure ratio	15	Kesser et al., 1994 [24]
	Polytropic efficiency (%)	89	
	Compressor air leakage (%)	1	Kesser et al., 1994 [24]
Turbine	Inlet temperature (°C)	1,308	Kesser et al., 1994 [24]
	Isentropic efficiency (%)	88	
Combustor	Efficiency (%)	100	
	Pressure drop (%)	3	Kesser et al., 1994 [24]
Fuel compressor	Polytropic efficiency (%)	89	
Reformer (REF)	Outlet pressure (bar)	19.2	Kesser et al., 1994 [24]
	Hot side pressure drop (%)	2	Kesser et al., 1994 [24]
	Code side pressure drop (%)	10	Kesser et al., 1994 [24]
	Minimum temperature difference (°C)	20	Kesser et al., 1994 [24]
Recuperator (REP)	Minimal temperature difference (°C)	20	
	Pressure drop for both cold and hot sides (%)	1	
HRSG	Minimal temperature difference (°C)	15	
	Hot side pressure drop (%)	2	Kesser et al., 1994 [24]
	Code side pressure drop (%)	5	Kesser et al., 1994 [24]
Pump	Efficiency (%)	85	
Economizer (ECO)	Minimum stack temperature (°C)	100	Kesser et al., 1994 [24]
stack	Exit pressure (bar)	1.013	Kesser et al., 1994 [24]
System	Mech. efficiency×generator efficiency (%)	98	
Solar collector	Solar heat temperature (°C)	~220	
	Solar collector efficiency (%)	72	
	Heat transfer efficiency (%)	95	

Table 2 Data summary for the computational model validation (the state point numbers refer to Fig. 2)

	Kesser et al. [24]	Case A
Compressor inlet (state point 1 in Fig. 2)		
m_1 (kg/s)[a]	1.0	1.0
T_1 (°C)[a]	15	15
p_1 (bar)[a]	1.0	1.0
Turbine inlet (state point 10 in Fig. 2)		
m_{10} (kg/s)	0.936	0.933
T_{10} (°C)	1308	1308
p_{10} (bar)[a]	14.55	14.55
Turbine exit (state point 11 in Fig. 2)		
m_{11} (kg/s)	1.155	1.156
T_{11} (°C)	596	589.5
p_{11} (bar)[a]	1.05	1.05
Reformer		
Chemical equil. approach temp. diff., ΔT_{eq} (°C)[a]	3.6	3.6
Minimal heat transfer temp. diff., ΔT_p (°C)[a]	20	20
Reformer exit (state point 9 in Fig. 2)		
m_9 (kg/s)	0.165	0.166
T_9 (°C)	576	569.5
p_9 (bar)[a]	19.2	19.2
CH_4 (mol %)	0.08	0.081
H_2 (mol %)	0.19	0.183
CO (mol %)	0.004	0.004
H_2O (mol %)	0.682	0.69
CO_2 (mol %)	0.044	0.043
Overall cycle parameters		
Water-methane mole ratio, R_{sm}[a]	6.1	6.1
Water-air mass ratio, X_s	0.144	0.145
Blade cooling air fraction, X_{bc}	0.219	0.222
Specific power output (kJ/kg air)	516.1	513.7
Thermal efficiency (%)	48.8	48.6

[a]Input data to the calculation.

where W_{net} is the net electric power produced by the SOLRGT system and $Q_f = m_f LHV$ is the fuel low heating value input, Q_{sol} is the absorbed solar heat by steam generation.

Since the system inputs consisting of the methane chemical energy and solar heat different in their energy qualities, exergy rather than energy efficiency is more suitable for the system performance evaluation. To be consistent with the thermal efficiency of the conventional CRGT cycle without solar heat input, an equivalent exergy efficiency η_e is defined in Eq. (25) as follows, assuming that the methane exergy is approximately equal to its lower heating value *LHV*; in addition, the exergy of the solar heat at a temperature of T_{sol} is calculated as the maximal work availability between T_{sol} and the ambient temperature T_0, i.e., is $Q_{sol}(1 - T_0/T_{sol})$. When solar input Q_{sol} is zero, η_e is equal to the thermal energy efficiency (such as in a conventional fossil fuel power plant), and is called system efficiency hereafter.

$$\eta_e = \frac{W_{net}}{Q_f + Q_{sol}(1 - T_0/T_{sol})} = \frac{W_{net}}{m_f \cdot LHV + Q_{sol}(1 - T_0/T_{sol})} \tag{25}$$

The contribution of the low/mid temperature level solar heat can be measured by its share in the system total energy input:

$$X_{sol} = \frac{Q_{sol}}{Q_f + Q_{sol}} = \frac{Q_{sol}}{m_f \cdot LHV + Q_{sol}} \tag{26}$$

The solar exergy share therefore is:

$$X_{e,sol} = \frac{Q_{sol}(1 - T_0/T_{sol})}{m_f \cdot LHV + Q_{sol}(1 - T_0/T_{sol})} \tag{27}$$

To indicate the role of the solar heat contribution in the proposed SOLRGT system, we adopt from Ref. [16] the definition of the net solar-to-electricity efficiency, η_{sol}, as:

$$\eta_{sol} = \frac{W_{net} - W_{ref}}{Q_{rad}} = \frac{W_{net} - Q_f \eta_{e,ref}}{Q_{rad}} \tag{28}$$

in which W_{ref} is the power output generated by a reference system, here it is chosen to be the conventional intercooling CRGT system (IC-CRGT) with the same methane input, $W_{ref} = Q_f \cdot \eta_{e,ref}$; Q_{rad} represents the total solar energy incident on the solar concentrator, $Q_{rad} = Q_{sol}/(\eta_{col} \cdot \eta_{tr})$, and where η_{col} is the concentrating solar collector efficiency, η_{tr} is the heat transfer efficiency from the collector to the cycle working fluid.

The fossil fuel savings in comparison with the conventional IC-CRGT power plant, for generating the same amount of electricity, is defined as the fossil fuel saving ratio:

$$SR_f = \frac{W_{net}/\eta_{e,ref} - Q_f}{W_{net}/\eta_{e,ref}} = 1 - \frac{W_{ref}}{W_{net}} \tag{29}$$

5.2 System Performance and Discussions. The SOLRGT system described in Fig. 3 is simulated using the same assumptions used for the CRGT (Case A) simulation. The fuel and the water mass flow rates are varied proportionally to maintain the same steam/methane ratio of 6.1, to match the combustor exit temperature of 1308 °C. Table 3 shows the parameters of the stream state points. For the system performance comparison, the reference system the intercooling CRGT cycle (IC-CRGT, referred to as Case B) is simulated as well with the same assumptions shown in Table 1, including the *TIT* of 1308 °C and compressor inlet air flow rate of 1 kg/s and so on. The performance of the three systems are compared and summarized in Table 4.

Case B, the intercooling CRGT system (IC-CRGT) was chosen as the reference system without solar assist to calculate the solar-to-electricity efficiency and fossil fuel saving ratio in the SOLRGT system. We observed that the solar heat used in the SOLRGT cycle contributes 20.3% of the system total energy input, leading to an 18.9% reduction of fossil fuel demand for producing the same amount of electricity. Notably, it achieves a net solar-to-power efficiency of 29.1% with the solar thermal energy

Table 3 Main stream states of the SOLRGT system (the state point numbers refer to Fig. 3)

				Molar composition (%)						
No.	T (°C)	p (bar)	m (kg/s)	CH_4	H_2	CO	CO_2	H_2O	O_2	N_2
1	25	1.013	1						21	79
2	183.4	3.87	1						21	79
3	30	3.83	1						21	79
4	194.9	15	0.832						21	79
5	491.3	14.86	0.832						21	79
6	25	2	0.141					100		
7	25	22.49	0.141					100		
8	218.2	22.39	0.141					100		
9	215.8	21.38	0.141					100		
10	25	5.0	0.021	100						
11	152.3	21.33	0.021	100						
12	206.7	21.33	0.162	14.1				85.9		
13	491.3	21.12	0.162	14.1				85.9		
14	575.7	19.2	0.162	7.9	18.9	0.4	4.4	68.4		
15	1308	14.55	0.994				3.4	27.4	9.2	60
16	595.7	1.05	1.162				2.9	23.7	10.8	62.6
17	511.3	1.03	1.162				2.9	23.7	10.8	62.6
18	248.1	1.02	1.162				2.9	23.7	10.8	62.6
19	163.3	1.01	1.162				2.9	23.7	10.8	62.6

Note: based on 1 kg/s compress or inlet air flow rate, steams for blade cooling are not listed in the table.

Table 4 Cycles performance comparison

	CRGT Case A	IC-CRGT Case B	SOLRGT Case C
Compressor inlet air mass flow rate m_1 (kg/s)	1.0	1.0	1.0
Fuel to air mass ratio	0.021	0.026	0.02
Reformer exit temperature (°C)/pressure (bar)	569.5/19.2	579.4/19.2	575.7/19.2
Water-to-methane mole ratio, R_{sm}	6.1	5.02	6.1
Methane conversion rate, CR	0.365	0.340	0.378
Steam-to-air mass ratio, X_s	0.145	0.145	0.14
Blade cooling air fraction, X_{bc} (%)	22.2	17.1	16.8
Solar thermal share, X_{sol} (%)	—	—	20.3
Solar-to-power efficiency, η_{sol} (%)	—	—	29.1
Fossil fuel saving ratio, SR_f (%)	—	—	18.9
Specific CO_2 emission (g/kWh)	406.4	422.7	343
Specific net power output, W_{net} (kJ/kg air)	513.7	601.9	592.6
Thermal efficiency, η_{th} (%)	48.6	46.7	45.9
System efficiency, η_e (%)	48.6	46.7	52.3

input at ~220 °C. The specific CO_2 emission of SOLRGT is 343 g/kWh, lower by 15.6% and 18.9% than that emitted by the basic CRGT and IC-CRGT systems, respectively. As expected, the relative reduction of CO_2 specific emission is equal to the fossil fuel saving ratio, SR_f, because the CO_2 emission is proportional to the fossil fuel consumption. The performance presented in Table 4 is the peak value with the optimal solar collector temperature. If the solar heat temperature is lower than the desired value of ~220 °C, then either a lower evaporation pressure should be chosen and a steam compressor is needed to elevate the steam pressure after the evaporation or some other complementary heat sources or heat storage is needed, resulting to the worsening of the efficiency and the other performance criteria in both cases.

Compared with the basic CRGT, both the IC-CRGT and SOLRGT systems employ compressor intercooling, resulting in a lower need for turbine blade cooling (by 23% in IC-CRGT and 24.8% in SOLRGT), and in significant specific power generation increase (by 17.2% in IC-CRGT and 15.4% in SOLRGT). The associated slightly increased turbine exit temperature with reduced blade cooling is also favorable to methane conversion. In the IC-CRGT system, however, the lower compressor outlet temperature resulting from intercooling increases the fuel demand. To maintain the same steam-methane ratio as that in the basic CRGT system, the steam flow rate needs be increased proportionally. However, for a given turbine inlet temperature and expansion ratio, the turbine exhaust heat is insufficient for generating the additional amount of steam needed. R_{sm} thus decreases to 5.0 in the IC-CRGT system, with this R_{sm} value attained by using the maximal steam generation rate allowable by the pinch point constraint in the HRSG. The lower R_{sm} decreases the methane conversion rate in the reformer, thus resulting in further lowering of the efficiency in the IC-CRGT system. In the SOLRGT system, however, the situation is different: with low/mid temperature solar heat input for steam generation, the pinch-point constraint is eliminated and the same R_{sm} of 6.1 can be maintained and actually there is potential to produce even more steam than that. Production of sufficiently high steam rates, together with the slightly higher turbine exhaust temperature than that in the basic CRGT, elevate the methane conversion rate and increase the chemical recuperation of heat. In addition, turbine exhaust heat can be used for preheating the compressed working fluid instead of steam generation, thus offsetting the negative impacts of intercooling on efficiency and retaining its positive impacts of lower compression power consumption and lower blade cooling requirement. The SOLRGT system therefore exhibits better performance than both the CRGT and IC-CRGT systems. Its specific power output is, however, slightly lower than that of the IC-CRGT system because it demands less fuel (and thus less steam for a given R_{sm}, it is noteworthy that the SOLRGT system has the lowest steam-to-air mass ratio X_s among the three systems) and thus the working fluid flow in the turbine is lower.

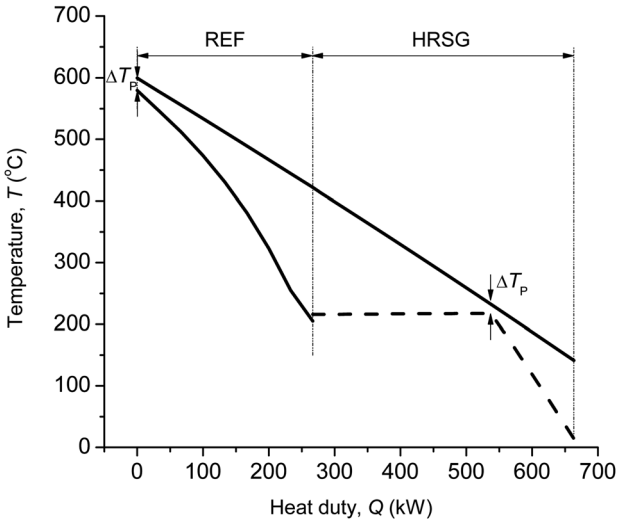

Fig. 4 Heat recuperation *T-Q* diagram for the IC-CRGT system

Figures 4 and 5 depict the temperature profile of the turbine exhaust heat recuperation in the IC-CRGT and SOLRGT systems, respectively. In both systems, the turbine exhaust heat is recovered in a high to low temperature cascade. In the SOLRGT system, the isothermal evaporation of the water is by the solar collector instead and thus the mid-level turbine exhaust heat provides just sensible heat for the variable temperature heat addition in the recuperator (REP). This achieves a good thermal match between the heating and heated streams exhibited by a more uniform temperature difference between them and reduces the related exergy destruction in the heat recuperation process.

5.3 Comparison of the SOLRGT With a Conventional Combined Cycle (CC) Power Plant. The gas/steam turbines combined cycle (CC) is the most efficient power generation system available commercially, it is used widely, and is reliable and economically competitive. It is therefore appropriate to compare the novel SOLRGT proposed and analyzed in this paper to the CC. Configurationally, both the SOLRGT and the CC use the exhaust heat from the topping gas turbine to improve the overall system efficiency: SOLRGT uses the exhaust heat to reform fuel to syngas, which is then used as the fuel in the gas turbine

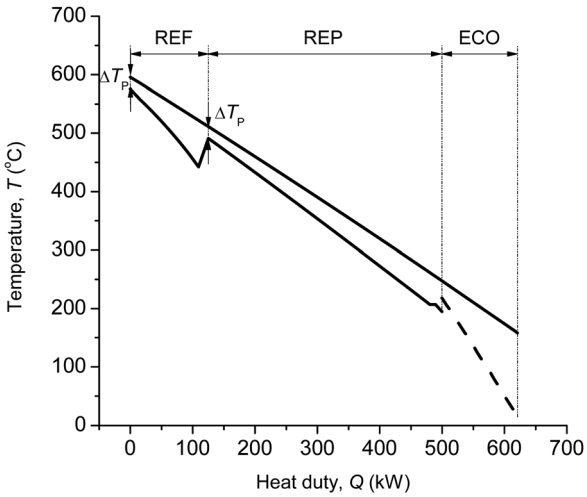

Fig. 5 Heat recuperation *T-Q* diagram for the SOLRGT system

combustor and CC uses it to generate steam for a bottoming Rankine-type cycle that generates additional power with its steam turbine. As explained in detail above, the reforming subsystem makes more efficient use of the source fuel exergy and also allows the use of lower temperature energy sources, such as solar in the SOLRGT, to contribute to the overall energy input and thus to reduce the use of fossil fuel and the associated undesirable emissions.

First we are comparing the performance of the SOLRGT and CC operating at the same *TIT*, based on fuel consumption alone. Further below we also discuss, qualitatively at this point, the hardware comparison, and the advantages of solar assist.

(1) Comparison of thermal performance:
For the purpose of this comparison we have calculated here the power generation efficiency η_f of the SOLRGT system, based on the fossil fuel input only, using the following definition:

$$\eta_f = \frac{W_{\text{net}}}{Q_f} \tag{30}$$

The CC reaches 60% efficiency for a *TIT* of 1430 °C (GE technology with close-loop steam cooling), and we could have chosen the same *TIT* for the SOLRGT analyzed in this paper, but we have chosen a *TIT* of 1300 °C to simplify the turbine and make it cheaper. We are therefore comparing our SOLRGT with a CC that has the same $TIT = 1300\,^{\circ}\text{C}$, where its efficiency is about 55%.
To compare with the common power generation efficiency of a combined cycle system operating at the same *TIT* of 1300 °C, which is 55%, a normalized efficiency is defined as

$$\eta_{f,\text{rel}} \equiv \frac{\eta_f}{\eta_{cc}} = \frac{\eta_f}{0.55} \tag{31}$$

Figure 6 shows η_f and $\eta_{f,\text{rel}}$ as a function of the solar thermal energy input fraction X_{sol} ($X_{\text{sol}} = Q_{\text{sol}}/(Q_f + Q_{\text{sol}})$) of the system.
Examining this figure shows that $\eta_{f,\text{rel}}$ becomes larger than 1.0 when the solar thermal fraction X_{sol} is above ~14%, indicating that the fuel-based efficiency of the SOLRGT with $X_{\text{sol}} > 14\%$ is higher than that of the CC system. If we were to simulate the SOLRGT for a *TIT* of 1430 °C and use a 60% efficiency for the CC, we would find that the fuel-based efficiency of the SOLRGT is again higher than that of the CC system, i.e., > 60%. As shown in Sec. 6 below, the maximal practical value of X_{sol} in the analyzed system is near 29%, indicating that the fuel efficiency of SOLRGT can be up to 13% higher than that of CC (corresponding to ~12% fossil fuel saving).

(2) Solar and environmental comparison:
Since the SOLRGT system uses up to 12% less fossil fuel than the CC (within the parameter range of this study), it commensurately reduces CO_2 emissions and saves the depletable fossil fuel. Furthermore, due to the introduction of steam into the combustion chamber, production of NO_x is near zero, lower than that of the CC.
Comments about the qualitative economic comparison between the systems are given at the end of Sec. 8

6 Parametric Analysis of the Solar Heat Input Ratio

In the SOLRGT system increasing solar heat input corresponds to increasing the steam addition. The steam-air mass ratio (defined as the ratio of solar heat generated steam mass flow rate and the compressor inlet air mass flow rate, i. e., $X_s = m_9/m_1$) is an important parameter for the system performance since higher steam addition means that there is a higher solar heat input, and thus raises the system efficiency η_e.

In the calculation above, the IC-CRGT system (Case B) already produces the maximal steam rate possible within the pinch point temperature difference constraint of 15 °C in the HRSG. In the basic CRGT system (Case A), the steam production rate is also near its maximum ($\Delta T_p = 17.6\,^{\circ}\text{C}$). In contrast, the steam generation rate in the SOLRGT system (with $X_s = 0.14$, the lowest among the three systems) is far below the maximum that can be produced from the solar and turbine exhaust recuperation heat, in which the constraint of the pinch point in evaporator is eliminated and replaced by the constraint of the lowest flue gas temperature leaving the system. The flue gas temperature at the exit of the economizer is 163 °C, above the minimally needed 100 °C stack temperature, indicating potential to produce more steam. Practically, the steam/air mass flow ratio is limited by the size of the turbine flow passages. Since we are aiming to investigate the potential of the systems, it is assumed the turbine is designed to accommodate the increased flow rate. Figures 7 and 8 represent a hypothetical family of SOLRGT systems with fixed compressor pressure and combustor outlet temperature, which have different solar heat input shares X_{sol}, by varying the steam/air ratios. The highest $X_{\text{sol}} = 0.288$ corresponds to the maximal steam production rate within the limits of the constraint on the lowest flue gas temperature at the economizer outlet, of 100 °C in this study.

Figure 7 shows the steam-air mass ratio X_s, the net solar-to-electricity efficiency η_{sol}, and the fossil fuel saving ratio SR_f. The

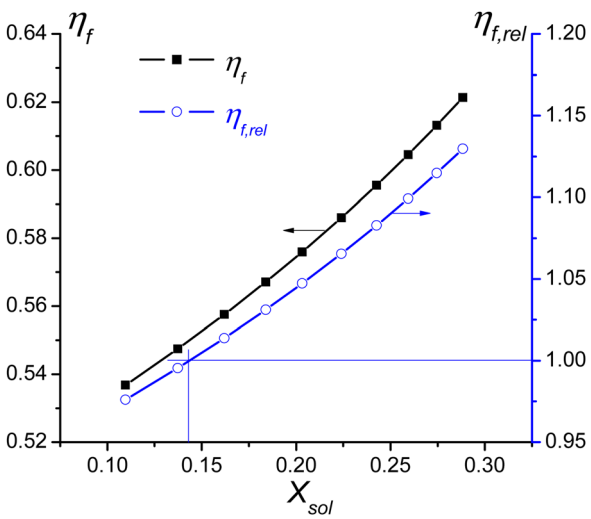

Fig. 6 Comparison of thermal performance with CC

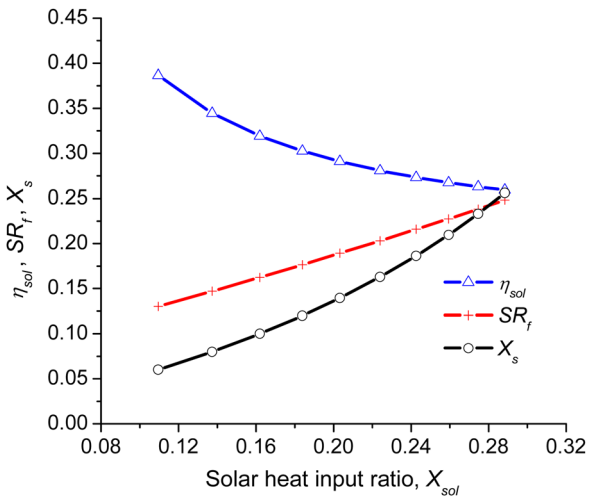

Fig. 7 The impact of solar thermal share X_{sol} on solar-to-electricity efficiency η_{sol}, and fossil fuel saving ratio SR_f

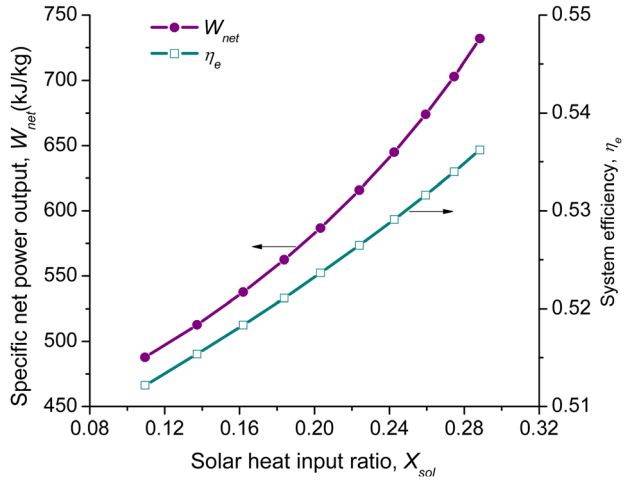

Fig. 8 The impact of solar thermal share X_{sol} on system efficiency η_e and specific net power output W_{net}

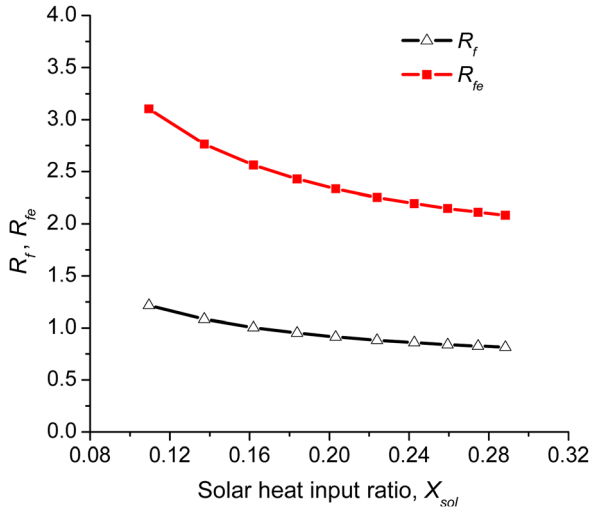

Fig. 9 The replacement of fossil fuel energy by solar thermal energy/exergy, R_f and R_{fe}

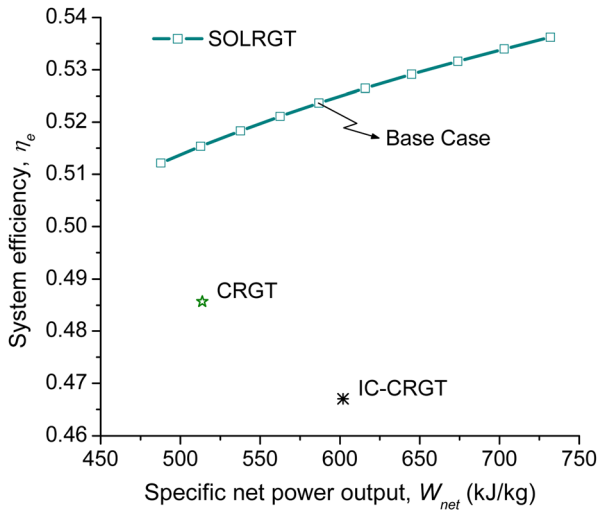

Fig. 10 System performance comparison

solar energy heat input share, employed to supply the vaporization latent heat, increases as more steam is being introduced to the system. The steam addition increases the turbine working fluid flow rate, and it also strengthens both the chemical and thermal energy recuperation and thus improves overall system performance. The increasing working fluid flow rate increases the power generation and the blade cooling demand. As more solar heat is brought into the system, more fossil fuel can be saved, and the system efficiency consequently increases. Figures 7 and 8 show that when X_{sol} is increased from 0.11 to 0.288 (i.e. 2.6-fold), the specific power based on the compressor inlet air increases from 488 kJ/kg to 732 kJ/kg (1.5-fold), the efficiency increases from 51.2% to 53.6% (1.05-fold), and the fossil fuel saving ratio increases from 13% to 25% (1.9-fold).

The only parameter which shows an undesirable variation with X_{sol} increase is the solar-to-electricity efficiency η_{sol}. The net solar-to-electricity efficiency reaches a remarkably high level of 38.7% at the lowest X_s of 0.06, with the lowest solar energy thermal share of 11%. As X_s is increased to 0.256, the solar thermal share increases to 28.8% while the solar-to-electricity efficiency drops to 26%.

It is interesting to notice that the fossil fuel energy saving ratio SR_f varies with the same tendency as the solar thermal input share X_{sol}.

From Eq. (26), we obtain:

$$Q_{sol} = \frac{X_{sol}}{1 - X_{sol}} Q_f \tag{32}$$

Using Eqs. (29) and (32), the replacement of fossil fuel by solar energy can be expressed as:

$$R_f = \frac{W_{net}/\eta_{e,ref} - Q_f}{Q_{sol}} = SR_f \cdot \frac{W_{net}/\eta_{e,ref}}{Q_f} \cdot \frac{Q_f}{Q_{sol}} = \frac{SR_f}{1 - SR_f} \frac{1 - X_{sol}}{X_{sol}} \tag{33}$$

Similarly, the replacement of fossil fuel by solar exergy can be obtained as:

$$R_{fe} = \frac{W_{net}/\eta_{e,ref} - Q_f}{Q_{sol}(1 - T_0/T_{sol})} = \frac{R_f}{(1 - T_0/T_{sol})} \tag{34}$$

Figure 9 shows the replacement of fossil fuel by solar energy/exergy, R_f and R_{fe}, respectively. It is found that R_f and R_{fe} have similar variation tendencies as that of η_{sol}, they decrease as the steam-air ratio X_s increases. For Case C with $X_s = 0.14$, R_f and R_{fe} are found to be 0.91 and 2.33, respectively. This implies that 1 kJ of low-quality solar heat input replaces 0.91 kJ of high-quality fossil fuel or 1 kJ of solar exergy input can replace 2.33 kJ of fossil fuel. This result shows very encouraging fossil fuel saving and the related pollution reduction in the new system. The SOLRGT system efficiency versus specific net power output is summarized in Fig. 10, in which the performance of the basic CRGT system (Case A) and the CRGT with intercooling (IC-CRGT, Case B) are also shown for comparison.

7 Technical Considerations

The technologies involved in SOLRGT, including the steam reforming and low/mid temperature solar heat collection, are all well established. Steam reforming is widely used in the chemical process industry for hydrogen or syngas production, as an intermediate step to further products such as ammonia or methanol. For the low temperature reforming in the CRGT cycle, low-cost methane-steam reforming catalysts that are effective at the temperature levels encountered in gas turbine exhausts are critical. The performance and size of a methane-steam reformer for a basic CRGT power plant was analyzed in Ref. [31]. The commercially mature parabolic trough solar collector [32] may be used to provide heat at ~220 °C for water evaporation. The thermal

efficiency of the current parabolic trough collector can reach above 50%, even with a low direct solar radiation of 100 W/m^2 and solar collector average temperatures below 200 °C [16]. It is worth pointing out that the significant improvement of the system efficiency and the solar-to-electricity efficiency directly contributes to the reduction of solar collector area and the solar field size, and the better exploitation of the turbine exhaust heat in this novel SOLRGT system further reduces the solar heat share and the related collector size, as shown in Part II [33] of this study.

The environmental issues should also be taken into account when evaluating the system performance. The formation of nitrogen oxides (NO_x) during combustion is a main pollutant problem associated with gas turbine power generation. The presence of a significant quantity of steam in the hydrogen-enriched syngas in the CRGT system lowers the flame temperature resulting in potential ultra-low NO_x emissions, eliminating the need for using low-NO_x combustion technologies. The environmental benefits of the solar-assisted hybrid system due to CO_2 mitigation and other pollution abatement associated with its fossil fuel saving contribute to its economic competitiveness with conventional power systems.

8 Economic Analysis

To evaluate the economic performance of the SOLRGT system, an approximate economic analysis is conducted that calculates the cost of produced electricity and the system payback period by taking into account (1) all expenditures over the life of the system from construction start till end of useful life, with the expenditures composed of the estimated initial (one-time) capital investment, fuel (here methane), and O & M costs, and the cost of money (discount rate) assuming that 50% of the initial capital was borrowed at the discount rate, and (2) the electricity generated by the system, computed from the system performance simulation described, as well as the average price of electricity, both over its life. The following assumptions were made for the base case estimation:

- The price of methane is constant at 0.144 \$/Nm^3 for power generation [34].
- The plant operation life n is 30 years [35–39].
- The interest rate i is constant at 8% [40,41].
- The price of the land for the plant is 2.8 \$/m^2 [38].
- The annual O & M (cost of operation and maintenance), is constant at 4% of the investment capital cost of the system [40,41].
- The construction period is two years, so the total life time is 32 years. It is assumed, similar to other, power plant funding assumptions (e.g Ref. [42]) that 50% of the total investment cost is an interest-bearing loan and the other 50% is equity, and a loan interest rate of 8%, and the loan period (years) which is assumed to be equal to the system operation life, which means there is no loan payment during the construction period [40,41].
- The annual operating time H of the hybrid system depends on the capacity of the solar heat subsystem. A thermal storage system is adopted to prolong the availability of the solar heat and thus the operation hours. Fuel complementary combustion is not considered in this calculation.

Table 5 Size of the hybrid system under evaluation (design state performance)

Plant components	Capacity
Power block (MW_e)	361
Solar heat input Q_{sol} (MW_{th})	160.2
Air mass flow rate (kg/s)	610
Methane flow rate (kg/s)	12.5
Water flow rate (kg/s)	86.0
Reformer (MW_{th})	77.2
Economizer (MW_{th})	71.2
Recuperator (MW_{th})	230.4
Intercooler (MW_{th})	96

The analysis is for a hybrid system of 361 MWe net capacity, as reported in Table 5.

Some other relevant assumptions are summarized in Table 6.

8.1 Evaluation of the Total Plant Cost (*TPC*). The total plant cost (*TPC*) estimation of the hybrid systems is presented in Table 7. The *TPC* consists of the equipment and balance of plant (*BOP*) costs. The *BOP* covers the remaining systems, components, and structures that comprise a complete power plant or energy system that is not included in the prime mover. For a power generation system, the *BOP* is usually assumed to be 15% of the known components' cost [40–42,47].

In the solar subsystem of SOLRGT, the solar field is assumed to be installed with the SEGS (Solar Energy Generating Systems) LS-2 parabolic trough solar collectors, and the heat transfer fluid (HTF) is assumed to be Therminol VP-1 synthetic oil (Vapor Phase/Liquid Phase heat transfer fluid by Solutia) [35–38,48]. The direct solar radiation (*DNI*) of 944.5 W/m^2 refers to the measured value at noon in the summer solstice day [44].

The solar heat demanded by the power system at the nominal condition is:

$$Q_{sol} = Q_{rad} \cdot \eta_{col} \cdot \eta_{tr} \tag{35}$$

Q_{rad} is defined as total solar energy incident on the solar concentrator. η_{col} is the efficiency from solar to heat in HTF, and η_{tr} is the efficiency from heat in HTF to heat in working fluid of power cycle.

Thermal storage section is included using molten salt as the heat storage medium [35–38]. The solar multiple (*SM*) is defined as the ratio between the heat collection capacity of the solar field at the design point and the heat demand from the SOLRGT system at nominal conditions [36,37]:

$$SM = (Q_{th,solar\ field}/Q_{rad})\big|_{design\_point} \tag{36}$$

This parameter represents the solar field size and is directly related with the daily operation hours of the solar thermal storage section.

The cost of the solar field is evaluated as the area multiplied by its unit price. Taking the thermal storage system into consideration, the collector area is calculated as:

Table 6 Main assumptions for the calculation of the parabolic trough solar collector section

Solar collector	Parameters	Value	Source
Design point	Solar collector temperature (°C)	~250	H. Hong et al. 2005 [17]
	Solar collector design efficiency η_{col} (%)	72	Odeh et al. 1998 [43]
	Direct solar radiation *DNI* (W/m^2)	944.5	TRNSYS, 2010 [44]
	Solar multiple *SM*	1.4	Robert Pitz-Paal, 2005 [38]
	Heat transfer efficiency η_{tr} (%)	95	Robert Pitz-Paal, 2005 [38]
Annual value	Annual solar radiation *I* (kWh/(m^2·a))	2717	[36,37,44]
	Annual average collector efficiency $\bar{\eta}_{col}$(%)	48	[36–38,45,46]

$$S_{col} = \frac{Q_{rad}}{DNI} \cdot SM = \frac{Q_{sol}}{DNI \cdot \eta_{col} \cdot \eta_{tr}} \cdot SM \quad (37)$$

The annual running time of the hybrid system, H, is calculated as:

$$H = S_{sol} \cdot I \cdot \bar{\eta}_{col} \cdot \eta_{tr} / Q_{sol} = SM \cdot I \cdot \bar{\eta}_{col} / (\eta_{col} \cdot DNI) \quad (38)$$

where $\bar{\eta}_{col}$ is the annual average collector efficiency. The H of the SOLRGT system is found to be 2914 h/a.

The estimation of other component costs is explained in the footnotes of Table 7.

8.2 Evaluation of the Electricity Cost (*COE*) and Payback Period (*PBP*). The cost of electricity *COE* is calculated as,

$$COE = (\beta \cdot TPC + C_{om} + C_f) / (H \cdot W_{net}) \quad (39)$$

in which β is the annual average investment coefficient, a function of the interest rate i and plant operation life n:

$$\beta = i / [1 - (1+i)^{-n}] \quad (40)$$

C_{om} is the annual O &M cost of the systems. It covers both fixed and variable parts. Fixed O & M consists primarily of plant operating labor. Variable O & M includes periodic inspection, replacement, and repair of system components (i.e., solar collector, turbine, etc.), as well as consumables (i.e., water, catalyst, etc.) [40–42,47,50]. C_f is the annual fuel cost of the hybrid systems; W_{net} is the power output.

The payback period *PBP* is the time by which the current value of all the revenue becomes equal to that of the investment *TPC* [40,41]:

$$R \cdot [(1+i)^{PBP} - 1] / [i(1+i)^{PBP}] = TPC \quad (41)$$

where R is the annual net revenue of the plant:

$$R = R_e - C_f - C_{om} \quad (42)$$

R_e is the annual revenue of the net power product ($), defined as the electricity output multiplied by the electricity price, the latter defined here as the portion of the average retail price of electricity to ultimate customers (*RPE*) that is available to the plant owners, $/kWh.

Obviously, the value of *RPE* changes with time, sometimes abruptly/unpredictably, but more than that, we note that its determination is somewhat complex because it also depends on the regulations at the plant site, which change not only from country to country but also by site in a given country. This may lead to prices to the customer that are much lower than the generation cost, when national or local governments choose to subsidize electricity for socio-political or economic development reasons, or much higher than the cost when they choose to tax it for curbing demand or other reasons. A telling example is that in 2009, the household price of electricity ($/kWh) in the OECD was 0.156, ranging from 0.133 in Norway to 0.365 in Denmark, and 0.115 in the US [51]. Since electricity subsidies and taxes are beyond the scope of this study, and noting that the customer price in the US has in the period of 2000 to 2009 steadily increased for households from 0.081 to $0.115/kWh and for industry from 0.048 to $0.068/kwh, we have assumed that the base case *RPE* for calculating the payback period (*PBP*) is $0.08/kWh [51–53].

8.3 Economic Performances and Discussions. Table 8 presents the economic analysis results of the SOLRGT hybrid system, calculated by using the above-shown equations. With a thermal solar share of 20.3%, the *COE* (cost of the electricity) is 0.059 $/kWh and the *PBP* (payback period) is 10.7 years (including two years of construction). It thus shows that the SOLRGT is an economically feasible and even attractive choice for solar-assisted heat power generation.

The *COE* is composed of annual average investment, annual fuel cost (C_f) and annual O & M cost (C_{om}). The fuel cost constitutes the largest part of the *COE* (42.5%), closely followed by the

Table 7 Total plant cost (*TPC*) estimation of the SOLRGT system (based on the value of $ in 2009)

Plant components	Price and source	Capacity	Investment cost	Percentage
SOLRGT				
Simple cycle section[a]	228$/kW [49]	361 MW	82.2 M$	31.0%
Reformer[b]	—	77.2 MW_{th}	4.9 M$	1.9%
Economizer[c]	97$/$m^2$ [40,41]	0.0145 km^2	1.4 M$	0.5%
Recuperator[c]	244$/$m^2$ [40,41]	0.0440 km^2	10.7 M$	4.0%
Intercooler[c]	97$/$m^2$ [40,41]	0.0231 km^2	2.3 M$	0.9%
Power block (*BOP* included)	—	—	116.6 M$	44.0%
Solar field[d]	288.4$/$m^2$ [35]	0.3487 km^2	100.6 M$	37.9%
Thermal storage system[e]	12.06$/MJ [36]	1917 GJ	23.1 M$	8.7%
Solar evaporator[f]	5.6$/$kW_{th}$ [37,39]	168.6 MW_{th}	0.9 M$	0.3%
Solar block (*BOP* included)	—	—	143.3 M$	54.0%
Land cost[g]	2.8$/$m^2$ [38]	1.357 km^2	5.3 M$	2.0%
Total plant cost	—	—	265.3 M$	100.0%
Specific cost	—	—	736 $/kW	—

[a]The combustor, gas turbine, generator, and compressors are included. The unit cost is taken from the simple cycle specifications of the PG9351FA model (GE company, 50 Hz) [49].
[b]The Ni-based catalyst is filled inside. As the reforming reaction is in the moderate-temperature range, the unit cost of the reformer is much lower than that of the high-temperature reforming reactor in traditional hydrogen-production process. The cost is calculated with formula $C = C_0[Q/(Q_0)]^f$, where C_0 (39.8 M$) is the cost of the reference component (reformer) of size Q_0 (1377 MW_{th}), and f is the scale factor 0.67 [40,41].
[c]The heat transfer area of each component is calculated with formula $Area = Q/(U \cdot \Delta T)$. The heat duty Q and temperature approaches ΔT (taken as the mean logarithmic temperature difference) are taken from the simulation cases in ASPEN PLUS. The heat transfer coefficients U, for the economizer, recuperator and intercooler are 70, 150 and 70 W/(m^2K), respectively, which and the heat exchanger unit costs are taken from the research in Refs. [40, 41].
[d]The solar field cost includes parabolic trough solar collectors and HTF system (include heat transfer fluid and accessories) [35–39,48].
[e]The nitrate salt inventory, tanks and oil-to-salt heat exchanger are included, the heat storage efficiency $\eta_{st} = 0.95$ [38], the storage capacity achieves 3 h with the solar multiple *SM* of 1.4, its heat storage capacity is thus $3Q_{sol}/(\eta_{tr} \cdot \eta_{st})$ X3600 = 1917 GJ [38].
[f]The capacity is the heat duty of the oil-to-water heat exchanger, Q_{sol}/η_{tr}.
[g]The total area of the plant is amplified proportionally from the solar field area by 3.891 folds [38].

Table 8 Economic performances of the SOLRGT system (base case.2009 $)

SOLRGT items	Values
Thermal solar share X_{sol}, (%)	20.3
Annual operating time H, (h)	2914
Total plant cost TPC, (M$)	265.3
Construction interest, (M$)	22.1
Total plant investment, (M$)	287.3
Annual average investment, (M$)	25.5
Annual fuel cost (C_f), (M$)	26.5
Annual O&M cost (C_{om}), (M$)	10.4
Annual net revenue (R), (M$)	47.1
Specific Investment, ($/kW)	736
COE, ($/kWh)	0.059
PBP, (y)	10.7

annual average TPC part (40.9%), and the O & M (operation and maintenance cost) part is a little less, accounting for 16.7% of the total electricity cost. For the TPC part, the investments of the solar field and simple-cycle subsystems have the most important shares. It is thus obvious that the most effective ways to decrease the COE of SOLRGT would be in improving the system thermal efficiency (so as to cut down the fuel cost) and reducing the system cost, which is in any case going to follow the rising technical maturity of the solar heat collectors and power generation components.

8.4 Parametric Sensitivity Analyses. The influence of the solar heat share X_{sol} is examined below. It is varied by varying the input water mass flow rate under the constant gas turbine inlet temperature and compressor inlet air mass flow rate; as a result, fuel mass flow rate will change accordingly. The influences of other sensitivity factors, including solar collector efficiency η_{col}, fuel price, electricity price, O & M cost, simple-cycle unit price and solar field unit price, are analyzed individually, assuming that all the other parameters are invariable.

In Fig. 11, it is shown that the most significant factors that influence COE (cost of the electricity) are fuel price and solar collector efficiency η_{col}, and then followed by the solar heat share X_{sol}, solar field unit price, simple-power cycle unit price and O & M cost.

When η_{col} increases from 57% to 72%, the COE decreases from 0.0633 $/kWh to 0.0594 $/kWh. It illustrates the reason for choosing low/mid-temperature solar heat in SOLRGT system, to gain high solar collector efficiency and better system economic performances. A bigger solar heat share X_{sol} or solar field unit price

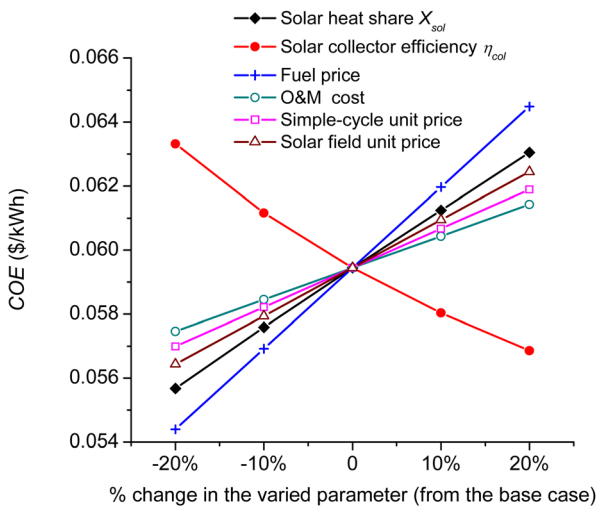

Fig. 11 Parametric sensitivity analyses of electricity cost *COE*

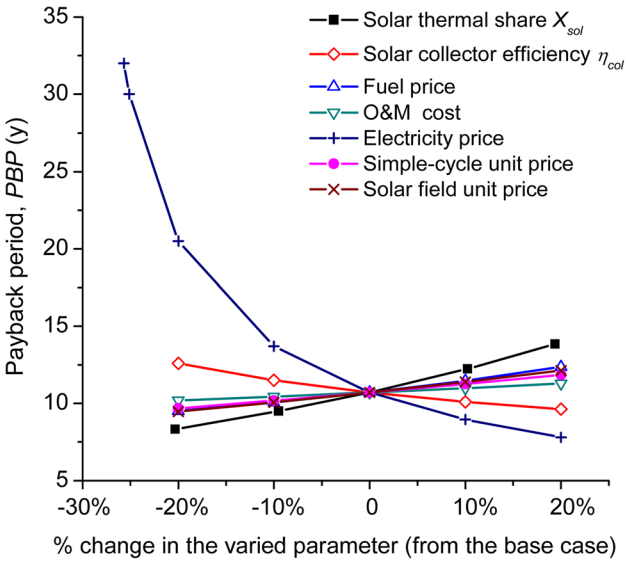

Fig. 12 Parametric sensitivity analyses of payback period *PBP*

raise COE. Therefore, the room for COE improvement mainly comes from the increase of η_{col} and decrease of solar field and simple-cycle unit costs.

In Fig. 12, the most important sensitivity factors for PBP (payback period), is the electricity sale price RPE; the solar heat share X_{sol} and solar collector efficiency η_{col} are second in significance. The fuel price, the solar field unit price, simple-cycle unit price and O & M cost have weaker influences.

When the electricity sale price RPE drops from the assumed RPE of 0.080 $/kWh to the calculated COE of 0.059 $/kWh, equivalent to a 25.1% drop in RPE, the PBP will rise to 32 years (including of two years of construction). In this case, the sum of the revenues during the plant operation life (30 years) just balances the investment TPC of SOLRGT. Electricity sale price RPE lower than COE obviously cannot recover the payment within the plant life time. It is thus shown that the economic benefit of the SOLRGT system is mostly dependent on the electricity pricing by the relevant authority.

The X_{sol}, η_{col} and solar field unit price affect the solar block investment, and thus have strong influences on the TPC and eventually on the PBP. The improvement of η_{col} would shorten the PBP markedly. The variation of fuel price and O & M cost alter the PBP via the system annual revenue but their influences are much smaller.

Again, we would like to have a comparison with the corresponding combined cycle power system at the same TIT level. Of course, a thorough thermo-economic analysis is needed for ultimate comparison, between the systems, which we haven't performed yet, but some preliminary comments can be made. Compared with the CC, the SOLRGT requires the reforming subcomponents and the solar collection system, but does not require the CC entire bottoming steam system. Since the SOLRGT solar collectors supply the heat at only 220 °C, they are not too expensive and are widely in use.

We note that the proposed system would have a large economic advantage over a system that uses only solar collectors at 220 °C without the hybridization (as most of the existing solar thermal power systems do), since the net efficiency of such a solar system is 7–10% only, and would require a huge and expensive solar collector field.

9 Concluding Remarks

The utility of indirect upgrading of low/mid-level solar energy and its high efficiency conversion to electricity is explored based

on the "energy level" concept, and is demonstrated by system integration of a hybrid solar improved CRGT (SOLRGT) system, in which the solar heat collected at the mid-level temperature of about 220 °C is first transformed into the latent heat of the vapor used in reforming natural gas to syngas, and then to the syngas chemical exergy. The solar heat-generated steam helps to improve both the chemical and thermal recuperation in the system, and enables a configuration with compression intercooling and recuperation (for preheating the compressed air). The net solar-to-electricity efficiency, based on gross solar thermal energy incident on the collector, is predicted to have an average value of 25–30%, and it can reach up to 38% with a reduced solar heat share. A fossil fuel saving of 20% is feasible with a solar thermal share of 22%, and the system overall efficiency reaches 51.2% to 53.6% as the solar heat share is increased from 11 to 28.8% by raising the steam/air ratio. The overall efficiency is about 5.6%-points higher than a comparable intercooled CRGT system without solar assist. Due to the introduction of steam into the combustion chamber, production of NO_x is near zero, and the reduction of fossil fuel use results in a commensurate ~20% reduction of CO_2 emissions as compared with the comparable intercooled CRGT system without solar assist. The system performance exhibits enhanced specific power output and efficiency and is very promising and comparable to the hybrid solar/methanol combined cycle power system proposed by Hong and Jin [16,17] and other power systems employing higher temperature solar energy [19].

Comparison of the fuel-based efficiencies of the SOLRGT and a conventional commercial CC shows that the efficiency of SOLRGT becomes higher than that of CC when the solar thermal fraction X_{sol} is above ~14%. At the maximal practical value of X_{sol} in the analyzed system (~29%), the fuel efficiency of SOLRGT can be up to 13% higher than that of CC. Since the SOLRGT system thus uses up to 12% less fossil fuel than the CC (within the parameter range of this study), it commensurately reduces CO_2 emissions and saves the depletable fossil fuel. Furthermore, due to the introduction of steam into the combustion chamber, production of NO_x is near zero, lower than that of the CC.

An economic analysis is also performed to identify the feasibility of SOLRGT and the results show that the *COE* of the system is about 0.059 $/kWh, and that the payback period is about 10.7 years (including the two years of construction) if the electricity sale price (*RPE*) has a commonly used and rational value of 0.08 $/kWh.

Acknowledgment

The authors gratefully acknowledge the important assistance of Dr. Chending Luo in the economic analysis, and the support of the Chinese Natural Science Foundation Projects (No. 51076152, 50836005) and the National Key Fundamental Research Project (No. 2010CB227301).

Nomenclature

A = energy level, $\Delta E/\Delta H$
A_b = blade surface area
A_g = flue gas path cross-sectional area
BOP = balance of plant costs (M$)
C = cost (M$)
COE = cost of electricity ($/kWh), Eq. (39)
C_P = specific heat (kJ/kg·K)
CR = methane conversion ratio
DNI = direct normal incident solar radiation (W/m^2)
E = exergy (kW)
EXL = exergy loss (kW)
H = entropy [kW]; annual running hours (h), Eq. (38)
I = annual solar radiation (kWh/(m^2·a))
i = interest rate
LHV = lower heating value of fuel (kJ/kg)
m = mass flow rate (kg/s)
n = plant operation life (y)
PBP = payback period (y)
p = pressure (bar)
Q = heat (kW)
R = annual revenue of the plant (M$), Eq. (42)
R_{sm} = steam-methane mole ratio to the reformer
R_f = fossil fuel replacement per kJ solar energy input (kJ fossil fuel/kJ solar heat), Eq. (33)
R_{fe} = fossil fuel replacement per kJ solar exergy input (kJ fossil fuel/kJ solar heat exergy), Eq. (34)
RPE = retail price of electricity ($/kWh)
S_{col} = collector surface area (km^2), Eq. (37)
SM = solar multiple, Eq. (36)
SR_f = fossil fuel saving ratio, Eq. (29)
St = stanton number
T = temperature (°C)
TIT = turbine inlet temperature (°C)
TPC = total plant cost (M$)
U = heat-transfer coefficient (W/(m^{2}K))
W_{net} = net power output (kW)
W_{ref} = power output of the reference system (kW)
X_{bc} = blade cooling air fraction
$X_{e,sol}$ = solar exergy input share, Eq. (27)
X_s = steam-air mass ratio
X_{sol} = solar heat input share, Eq. (26)
β = annual average investment coefficient, Eq. (40)
ε_c = blade cooling efficiency (%)
η_{cc} = thermal efficiency of a combined cycle
η_{col} = collector efficiency (%)
η_e = system efficiency (%), Eq. (25)
η_f = power generation efficiency of the SOLRGT based on the fossil fuel input only, Eq. (30)
$\eta_{f,rel}$ = normalized power generation efficiency compared to CC having the same *TIT*, Eq. (31)
η_{sol} = solar-to-electricity efficiency [%], Eq. (28)
η_{th} = thermal efficiency (%), Eq. (24)
η_{tr} = heat transfer efficiency (%)
ϕ = cooling effectiveness, Eq. (23)

Subscripts

b = turbine blade
c = cooling, coolant
col = collector
ex = external heat source, turbine exhaust heat
f = fuel
g = gas
om = operation and maintenance
rec = reaction
ref = reference system
rad = solar radiation
s = steam
sg = steam generation
sol = solar heat
syn = syngas
th = thermal
tr = heat transfer
w = water
0 = environment state
1,2…19 = states on the cycle flow sheet

References

[1] Lior, N., 1977, "Solar Energy and the Steam Rankine Cycle for Driving and Assisting Heat Pumps in Heating and Cooling Modes," Energy Convers., **16**, pp. 111–123.
[2] Lior, N., and Koai, K., 1984, "Solar-Powered/Fuel-Assisted Rankine-Cycle Power and Cooling System: Simulation Method and Seasonal Performance," ASME Trans. J. Sol. Energy Eng., **106**, pp. 142–152.
[3] Koai, K., Lior, N., and Yeh, H., 1984, "Performance Analysis of a Solar-Powered/Fuel-Assisted Rankine Cycle With a Novel 30 hp Turbine," Sol. Energy, **32**, pp. 753–764.
[4] Lior, N., and Koai, K., 1984, "Solar-Powered/Fuel-Assisted Rankine Cycle Power and Cooling System: Sensitivity Analysis," ASME Trans. J. Sol. Energy Eng., **106**, pp. 447–456.

[5] Sherburne, D., and Lior, N., 1986, "Evaluation of Minimum Fuel Consumption Control Strategies in the Solar-Powered Fuel-Assisted Hybrid Rankine Cycle," Proceedings of the ASES Ann. Meeting, pp. 300–303.
[6] Jensen, C., Price, H., and Kearney, D., 1989, "The 'SEGS Power Plants: 1988 Performance," 1989 ASME International Solar Energy Conference, San Diego, CA.
[7] Kolb, J., 1995, "Evaluation of Power Production from the Solar Electric Generating Systems at Kramer Junction: 1988 to 1993," Proceedings of the Solar Engineering, - ASME Press, New York, Vol. 1, pp. 499–504.
[8] Cohen, G. H., and Kearny, O., 1994, "Improved Parabolic Trough Solar Electric Systems Based on the Segs Experience," Proceedings of the American Solar Energy Society Conference, pp. 147–150.
[9] Buck, R., Bräuning, T., Denk, T., Pfänder, M., Schwarzbözl, P., and Tellez, M., 2002, "Solar-Hybrid Gas Turbine-Based Power Tower Systems (REFOS)," Trans. ASME, **124**, pp. 2–8.
[10] Müller, H., Freng, S., and Trieb, F., 2004, *Concentrating Solar Power–A Review of Technology*, Ingenia Energy, **18**, pp. 43–50.
[11] Dersch, J., Geyer, M., Herrmann, U., Jones, S. A., Kelly, B., Rainer Kistner, R., Winfried Ortmanns, W., Pitz-Paal, R., and Price, H., 2004, "Trough Integration into Power Plants - A Study on the Performance and Economy of Integrated Solar Combined Cycle Systems," Energy, **29**, pp. 947–959.
[12] DESERTEC Foundation, 2009, "Clean Power from Deserts," http://www.desertec.org/
[13] Qu, H., Zhao, J., Yu, X., and Cui, J., 2007, "Prospect of Concentrating Solar Power in China—The Sustainable Future," Renewable Sustainable Energy Rev., **12**(9), pp. 2505–2514.
[14] Ondrey, G., 2009, "Solar's Second Coming," Chem. Eng., **116**(3), pp. 18–21.
[15] Li, J., 2009, "Scaling up Concentrating Solar Thermal Technology in China," Renewable Sustainable Energy Rev., Rev, **13**(8), pp. 2051–2060.
[16] Hong, H., Jin, H., Ji, J., Wang, Z., and Cai, R., 2005, "Solar Thermal Power Cycle With Integration of Methanol Decomposition and Middle-Temperature Solar Thermal Energy," Sol. Energy, **78**, pp. 49–58.
[17] Hong, H., Jin, H., Sui, J., and Ji, J., 2008, "Mechanism of Upgrading Low-Grade Solar Thermal Energy and Experimental Validation," ASME Trans. J. Sol. Energy Eng., **130**, 021014.
[18] Hong, H., Jin, H., and Liu, B., 2006, "A Novel Solar-Hybrid Gas Turbine Combined Cycle With Inherent CO_2 Separation Using Chemical-Looping Combustion by Solar Heat Source," ASME Trans. J. Sol. Energy Eng., **128**, pp. 275–284.
[19] Tamme, R., Buck, R., Epstein, M., Fisher, U., and Sugarmen, C., 2001, "Solar Upgrading of Fuels for Generation of Electricity," ASME Trans. J. Sol. Energy Eng., **123**, pp. 160–163.
[20] Abdallah, H., and Harvey, S., 2001, "Thermodynamic Analysis of Chemically Recuperated Gas Turbines," Int. J. Therm. Sci, **40**, pp. 372–384.
[21] Zhang, N., and Lior N., 2009, "Use of Low/Mid-Temperature Solar Heat for Thermochemical Upgrading of Energy, With Application to a Novel Chemically-Recuperated Gas-Turbine Power Generation (SOLRGT) System," Proceedings of the ASME 2009 International Mechanical Engineering Congress and Exposition, November 13–19, Lake Buena Vista, FL, Paper No. IMECE2009-13037.
[22] Ishida, M., and Kawamura, K., 1982, "Energy and exergy Analysis of a Chemical Process System With Distributed Parameters Based on the Energy Direction Factor Diagram," Ind. Eng. Chem. Process Des. Dev., **21**, pp. 690–695.
[23] Ishida, M., 2002, *Thermodynamics Made Comprehensible*, Nova Science, New York.
[24] Kesser, K. F., Hoffman, M. A., and Baughn, J. W., 1994, "Analysis of a Basic Chemically Recuperated Gas Turbine Power Plant," ASME J. Eng. Gas Turbines Power, **116**, pp. 277–284.
[25] Abdallah, H., Facchini, B., Danes, F., de Ruyck, J., 1999, "Exergetic Optimization of Intercooled Reheat Chemically Recuperated Gas Turbine," Energy Convers. Manage., **40**, pp. 1679–1686.
[26] Nakagaki, T., Ogawa, T., Hirata, H., Kawamoto, K., Ohashi, Y., and Tanaka, K., 2003, "Development of Chemically Recuperated Micro Gas Turbine," ASME Trans. J. Eng. Gas Turbines Power, **125**, pp. 391–397.
[27] Han, W., Jin, H., Zhang, N., and Zhang, X., 2007, "Cascade Utilization of Chemical Energy of Natural Gas in an Improved CRGT Cycle," Energy, **32**, pp. 306–313.
[28] Stecco, S. Facchini, B., 1989, "A computer Model for Cooled Expansion in Gas Turbines," Proceedings of the ASME Cogen-Turbo Symposium, Nice, France.
[29] Elmasri, M. A., 1986, "On Thermodynamics of Gas Turbine Cycles: Part 2 - A Model for Expansion in Cooled Turbines," ASME J. Eng. Gas Turbines Power, **108**, pp. 151–159.
[30] Aspen Plus®, Aspen Technology, Inc., 2009, Version 11.1, http://www.aspentech.com/.
[31] Adelman, S. T., Hoffman, M. A., and Baughn, J. W., 1995, "A Methane-Steam Reformer for a Basic Chemically Recuperated Gas Turbine," ASME J. Eng. Gas Turbines Power, **117**, pp. 16–23.
[32] Price, H., Lüpfert, E., Kearney, D., Zarza, E., Cohen, G., Gee, R., and Mahoney, R., 2002, "Advances in Parabolic Trough Solar Power Technology," ASME J. Sol. Energy Eng., **124**, pp. 109–125.
[33] Zhang, N., Lior, N., 2012, "Use of Low/Mid-Temperature Solar Heat for Thermochemical Upgrading of Energy, Part II: A Novel Zero-Emissions Design (ZE-SOLRGT) of the Solar Chemically-Recuperated Gas-Turbine Power Generation System (SOLRGT) guided by its Exergy Analysis," ASME J. Eng. Gas Turbines Power, Accepted.
[34] U.S. Energy Information Administration, 2010, "Natural Gas Weekly Update," http://www.eia.doe.gov/oog/info/ngw/ngupdate.asp 2010.9.30.
[35] Geyer, M., Lupfert, E., Osuna, R., Esteban, A., Schiel, W., Schweitzer, A., Zarza, E., Nava, P., Langenkamp, J., and Mandelberg E., 2002, "EURO TROUGH - Parabolic Trough Collector Family Developed and Qualified for Cost Efficient Solar Power Generation," Proceedings of 11st International Symposium on Concentrating Solar Power and Chemical Technologies, Zurich, Switzerland, Paper No. 2009102502.
[36] Herrmann, U., Kelly, B., and Price, H., 2004, "Two-Tank Molten Salt Storage for Parabolic Trough Solar Power Plants," Energy, **29**, pp. 883–893.
[37] Montes, M. J., Abánades, A., Martínez-Val, J. M., Valdes, M., 2009, "Solar Multiple Optimization for A Solar-Only Thermal Power Plant, Using Oil as Heat Transfer Fluid in the Parabolic Trough Collectors," Sol. Energy, **83**, pp. 2165–2176.
[38] Pitz-Paal, R., Dersch, J., and Milow, B., 2005, *European Concentrated Solar Thermal Road-Mapping*, The German Aerospace Center (DLR) Stuttgart.
[39] Price, H., 2003, "Assessment of Parabolic Trough and Power Tower Solar Technology Cost and Performance Forecasts," National Renewable Energy Laboratory, Golden, CO.
[40] Zhang, N., Lior, N., Liu, M., and Han W., 2010, "COOLCEP (Cool Clean Efficient Power): A Novel CO_2-Capturing Oxy-Fuel Power System With LNG (Liquefied Natural Gas) Coldness Energy Utilization," Energy, **35**, pp. 1200–1210.
[41] Liu, M., Lior, N., Zhang, N., and Han, W., 2009, "Thermoeconomic Analysis of a Novel Zero-CO_2-Emission High-Efficiency Power Cycle Using LNG Coldness," Energy Convers. Manage., **50**, pp. 2768–2781.
[42] Kreutz, T., Williams, R., Consonni, S., and Chiesa, P., 2005, "Co-Production of Hydrogen, Electricity and CO_2 from Coal With Commercially Ready Technology Part B: Economic Analysis," Hydrogen Energy, **30**, pp. 769–784.
[43] Odeh, S. D., Morrison, G. L., and Behnia, M., 1998, "Modeling of Parabolic Trough Direct Steam Generation Solar Collectors," Sol. Energy, **62**, pp. 395–406.
[44] TRNSYS, A TRaNsient Systems Simulation Program, version 16, http://sel.me.wisc.edu/trnsys/ 2010.9.30.
[45] García-Rodríguez, L., and Gómez-Camacho, C., 2005, "Thermo-Economic Analysis of a Solar Multi-Effect Distillation Plant Installed at the Plataforma Solar de Almeria (Spain)," Desalination, **122**, pp. 205–214.
[46] Caldés, N., Varela, M., Santamaría, M., and Saez, R., 2009, "Economic Impact of Solar Thermal Electricity Deployment in Spain," Energy Policy, **37**, pp. 1628–1636.
[47] Larson, E. D., and Ren, T., 2003, "Synthetic Fuel Production by Indirect Coal Liquefaction," Energy Sustainable Dev., **7**, pp. 79–102.
[48] Solutia, Inc., Therminol VP-1, http://www.therminol.com 2010.9.30.
[49] Gas Turbine World, 2009, *2009 Handbook*, Pequot Publishing, Inc., Fairfield, CT.
[50] The Energy of California, 2010, "Operation and Maintenance Costs," http://www.energy.ca.gov/distgen/economics/operation.html 2010.9.30.
[51] International Energy Agency, 2011, IEA Statistics - Electricity Information - 2011, Paris, France.
[52] U.S. Energy Information Administration, 2010, "Average Retail Price of Electricity to Ultimate Customers by End-Use Sector, by State," http://www.eia.doe.gov/electricity/epm/table5_6_a.html 2010.9.30 7.4.
[53] U. S. Energy Information Administration, 2010, "Average Retail Price of Electricity to Ultimate Customers by End-Use Sector," http://www.eia.gov/electricity/annual/pdf/table7.4.pdf.